Transport of 3-Fluoro-L-α-Methyl-Tyrosine by Tumor-Upregulated L-Type Amino Acid Transporter 1: A Cause of the Tumor Uptake in PET

Pattama Wiriyasermkul[1,2], Shushi Nagamori*[1], Hideyuki Tominaga*[3], Noboru Oriuchi[4], Kyoichi Kaira[5], Hidekazu Nakao[6], Takeru Kitashoji[6], Ryuichi Ohgaki[1], Hidekazu Tanaka[1], Hitoshi Endou[2], Keigo Endo[4], Hiroyuki Sakurai[2], and Yoshikatsu Kanai[1]

[1]Division of Bio-system Pharmacology, Department of Pharmacology, Graduate School of Medicine, Osaka University, Suita, Osaka, Japan; [2]Department of Pharmacology and Toxicology, Kyorin University School of Medicine, Mitaka, Tokyo, Japan; [3]Department of Molecular Imaging, Gunma University Graduate School of Medicine, Maebashi, Gunma, Japan; [4]Department of Diagnostic Radiology and Nuclear Medicine, Gunma University Graduate School of Medicine, Maebashi, Gunma, Japan; [5]Department of Medicine and Molecular Science, Gunma University Graduate School of Medicine, Maebashi, Gunma, Japan; and [6]Nard Institute, Ltd., Amagasaki, Hyogo, Japan

L-3-^{18}F-α-methyl tyrosine (^{18}F-FAMT) has been developed as a PET radiotracer for tumor imaging. Clinical studies have demonstrated the usefulness of ^{18}F-FAMT PET for the prediction of prognosis and the differentiation of malignant tumors and benign lesions. ^{18}F-FAMT exhibits higher cancer specificity in peripheral organs than other amino acid PET tracers and ^{18}F-FDG. The accumulation of ^{18}F-FAMT is strongly correlated with the expression of L-type amino acid transporter 1 (LAT1), an isoform of system L highly upregulated in cancers. In this study, we examined the interaction of 3-fluoro-L-α-methyl-tyrosine (FAMT) with amino acid transporters to assess the mechanisms of ^{18}F-FAMT uptake in PET. **Methods:** We applied in vitro assays using established mammalian cell lines stably expressing LAT1 or a non–cancer-type system L isoform LAT2. The inhibitory effect on L-^{14}C-leucine uptake and the induction effect on efflux of preloaded L-^{14}C-leucine were examined for FAMT and other amino acid tracers. FAMT transport was compared among cell lines with varied LAT1 expression level. **Results:** FAMT prominently inhibited LAT1-mediated L-^{14}C-leucine uptake in a competitive manner but had less of an effect on LAT2. In the efflux experiments, FAMT induced the efflux of preloaded L-^{14}C-leucine through LAT1, indicating that FAMT is transported by LAT1 and not by LAT2. Among amino acid–related compounds examined in this study, including those used for PET tracers, the compounds with an α-methyl group such as FAMT, 2-fluoro-L-α-methyl-tyrosine, 3-iodo-L-α-methyl-tyrosine, and L-α-methyl-tyrosine were well transported by LAT1 but not by LAT2. However, L-methionine, L-tyrosine, 3-fluoro-L-tyrosine, 2-fluoro-L-tyrosine, and O-(2-fluoroethyl)-L-tyrosine were transported by both LAT1 and LAT2, suggesting that the α-methyl moiety is responsible for the LAT1 selectivity of FAMT. FAMT transport rate and LAT1 protein level were well correlated, supporting the importance of LAT1 for the cellular uptake of FAMT. **Conclusion:** Distinct from other amino acid PET tracers, because of its α-methyl moiety, FAMT is selective to LAT1 and not transported by LAT2. This property of FAMT is proposed to contribute to highly tumor-specific accumulation of ^{18}F-FAMT in PET.

Key Words: 3-fluoro-L-α-methyl-tyrosine (FAMT); amino acid transporter; PET; cancer

The most widely used PET radiotracer for tumor imaging at the moment is ^{18}F-FDG, a glucose analog that accumulates in tumor cells via glucose transporters on the plasma membrane (1). However, the well-recognized limitation of ^{18}F-FDG PET is high uptake in inflammatory lesions and granulation tissues and high physiologic background uptake in some normal tissues, giving rise to false-positive diagnostic findings (2). Amino acid tracers that in general exhibit a more tumor-selective nature have been considered to overcome such disadvantages of ^{18}F-FDG PET (3). L-methyl-^{11}C-methionine (^{11}C-MET), the most commonly used amino acid PET tracer, and the well-studied O-(2-^{18}F-fluoroethyl)-L-tyrosine (^{18}F-FET), for example, show lower uptake in normal tissues and inflammatory lesions than ^{18}F-FDG (3). However, most of the amino acid PET tracers, including ^{11}C-MET and ^{18}F-FET, still suffer from various levels of physiologic background uptake (4,5). The nonnatural amino acid analogs that are highly selective to cancers and do not accumulate in normal tissues and non-cancer lesions would be beneficial for high-specificity cancer diagnosis with PET.

We developed L-3-^{18}F-α-methyl tyrosine (^{18}F-FAMT) as an amino acid PET tracer and showed that ^{18}F-FAMT

accumulates specifically in tumors, confirming its usefulness in the detection of cancers (6–11). Recent clinical studies demonstrated that ^{18}F-FAMT PET is useful for the prediction of prognosis in non–small cell lung cancer and the differentiation of malignant tumors from benign lesions (9–11). In addition, physiologic background in ^{18}F-FAMT PET is low, except in the kidneys and urinary bladder, which are in the excretion path of ^{18}F-FAMT (8). These findings let us speculate that ^{18}F-FAMT accumulates in cancer cells by the amino acid transporters specifically expressed in cancers and not by transporters of noncancer cells, whereas other amino acid tracers are taken up by the transporters of both cancer and noncancer cells. In fact, the accumulation of ^{18}F-FAMT in non–small cell lung cancer is strongly correlated with the expression of L-type amino acid transporter 1 (LAT1), an isoform of system L highly upregulated in many cancers (9,11).

System L is a Na^+-independent amino acid transport agency mediating the cellular uptake of large neutral amino acids. So far, 4 isoforms of system L transporters have been identified: LAT1, LAT2, LAT3, and LAT4 (12–15). LAT1 and LAT2 belong to the solute carrier 7 (SLC7) family and form heterodimers with a single-membrane–spanning glycoprotein, the heavy chain of 4F2 cell surface antigen (4F2hc/CD98hc/SLC3A2), to be functional on the plasma membrane (16). LAT3 and LAT4 belong to the SLC43 family and do not require 4F2hc (14,15). Among them, LAT1 is widely expressed in primary human tumors of various tissue origins, such as the brain, colon, lung, liver, thymus, ovary, and skin and cancer cell lines, in which it plays essential roles in the growth and survival of cancer cells (12,17–20). LAT1 is upregulated in malignant tumors, and its expression is associated with tumor proliferation, angiogenesis, and poor prognosis (9,11,19,20). In contrast, LAT2 expression is not detected in cancer cells but is widely found in normal tissues, including epithelia of the small intestine and kidney, and thus is regarded as a non–cancer cell type transporter (13,16). We previously found that the expression of LAT1 is an independent and significant factor for predicting a poor prognosis in patients with non–small cell lung cancer, suggesting that the prognostic significance of ^{18}F-FAMT uptake is closely related to LAT1 expression (10,19,20). Although it has been proposed that ^{18}F-FAMT is taken up into cancer cells by LAT1, there is no report that demonstrates the direct transport of FAMT by LAT1 and its kinetic properties. In this study, we examined the interaction of FAMT with the amino acid transporters to assess its mechanisms of uptake in PET.

MATERIALS AND METHODS

Materials

3-fluoro-L-α-methyl-tyrosine (FAMT) and 2-fluoro-L-α-methyl-tyrosine (2-FAMT) were synthesized with chiral phase-transfer alkylation (21) and electrophilic fluorination (6) by Nard Institute, Ltd. FAMT and 2-FAMT were identified by the analysis of [1]H-nuclear magnetic resonance (NMR) (ECX-400P; Jeol) and

high-performance liquid chromatography (LC-2010A HT; Shimadzu) as follows: FAMT: ^{1}H-NMR (D$_2$O/DCl, 400 MHz): d 1.39 (3H, s), 2.76 (1H, d, $J = 14.0$ Hz), 3.08 (1H, d, $J = 14.0$ Hz), and 6.76–6.90 (3H, m); and 2-FAMT: ^{1}H-NMR (D$_2$O/DCl, 400 MHz): d 1.36 (3H, s), 2.94 (2H, s), 6.50–6.55 (2H, m), and 6.96–7.00 (1H, m). The purities of the compounds determined on high-performance liquid chromatography were 99% and 99% enantiomeric excess for both FAMT and 2-FAMT. L-^{14}C-leucine (9.66 GBq/mmol) was from Moravek Biochemicals. Standard amino acids and L-α-methyl-tyrosine (AMT) were from Sigma-Aldrich. 2-Fluoro-L-tyrosine (2FT), O-(2-fluoroethyl)-L-tyrosine (FET), and 3-iodo-L-α-methyl-tyrosine (IMT) were from Advance Biochemical Compounds GmbH. 3-Fluoro-L-tyrosine (3FT) was from Tokyo Chemical Industry. Unless specially denoted, other chemicals were purchased from Wako Pure Chemical Industries. The chemical structures of compounds used in this study are presented in Figure 1.

Cell Cultures

The mouse renal proximal tubule cell line S2 stably expressing human LAT1 (S2-LAT1) or human LAT2 (S2-LAT2) was used in the present study (22). Using LAT1-specific high-affinity inhibitor KYT-0353 (23) and nonselective system L inhibitor 2-aminobicyclo-(2,2,1)-heptane-2-carboxylic acid inhibiting both LAT1 and LAT2 (16), we confirmed that L-leucine transport in S2-LAT1 and S2-LAT2 cells is mediated almost exclusively by human LAT1 and LAT2, respectively (data not shown). S2-LAT1 and S2-LAT2 cells were maintained as described previously (22) and used between the passages of 5 and 15, during which period no remarkable change was observed in the level of LAT1 and LAT2 expression determined by Western blot and in the transport activity
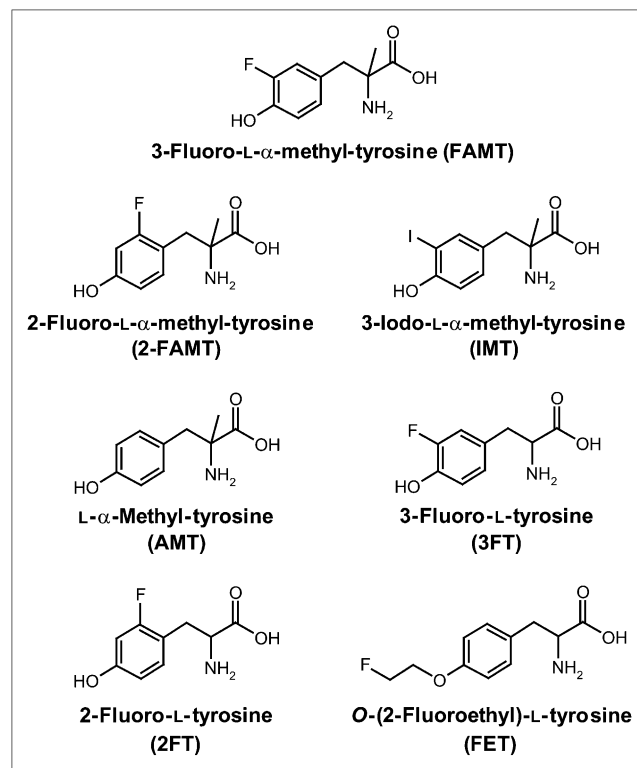

FIGURE 1. Chemical structures of compounds used in this study.

evaluated by L-^{14}C-leucine uptake. Human cell lines HEK 293 (embryonic kidney cell line), T24 (urinary bladder carcinoma), MIA PaCa-2 (pancreatic carcinoma), DLD-1 (colorectal adenocarcinoma), HeLa S3 (cervical adenocarcinoma), HEp-2 (HeLa subline), and H520 (non–small cell lung carcinoma cell line) were obtained from American Type Culture Collection. The cells were maintained by following the instructions from American Type Culture Collection.

Uptake Measurements and Inhibition Experiments

Uptake measurement was performed as described previously (22). The uptake of L-^{14}C-leucine by the cells was measured for 1 min in Na$^+$-free Hanks balanced salt solution ([HBSS]: 125 mM choline chloride, 4.8 mM KCl, 1.2 mM MgSO$_4$, 1.2 mM KH$_2$PO$_4$, 1.3 mM CaCl$_2$, 5.6 mM D-glucose, and 25 mM N-[2-hydroxyethyl] piperazine-N′-[2-ethanesulfonic acid], pH 7.4) containing L-^{14}C-leucine (5.0 MBq/mmol) at the concentration indicated in each experiment. For inhibition experiments, the uptake of L-^{14}C-leucine (1 μM) was measured for 1 min with or without nonradiolabeled test compounds at the indicated concentration. After uptake was terminated, the cells were lysed and the radioactivity was measured by a β-scintillation counter (LSC-3100; Aloka). An aliquot of the lysate was used to determine the protein concentration by bicinchoninic acid assay (Thermo Fisher Scientific).

The half maximal inhibitory effect (IC$_{50}$) of FAMT and 2-FAMT was determined by experiments in which the uptake of L-^{14}C-leucine (1 μM) was measured for 1 min in the presence of FAMT or 2-FAMT at concentrations of 1, 3, 10, 30, 100, 300, and 1,000 μM (24). The data were fitted to inhibition curves by nonlinear regression (4-parameter Hill function, SigmaPlot 11; Systat Software, Inc.).

The kinetic parameters of uptake inhibition by FAMT were determined on the uptake of L-^{14}C-leucine for 1 min at concentrations of 1, 2, 5, 10, 20, 50, and 100 μM (24). The uptake values in the presence or absence of 50 and 100 μM FAMT were plotted against L-^{14}C-leucine concentration and fitted to a Michaelis–Menten curve. The Michaelis constant (K$_m$) and the maximum velocity values (V$_{max}$) were determined by nonlinear regression (4-parameter Hill function). To obtain the inhibition constant (K$_i$), the rates of uptake of L-^{14}C-leucine were measured in the presence or absence of 50 μM FAMT. Double reciprocal plots were drawn using the enzyme kinetics module of SigmaPlot 11. The K$_i$ value was calculated by the following equation when competitive inhibition was observed: K$_i$ = concentration of FAMT/ ([K$_m$ of L-^{14}C-leucine with FAMT/K$_m$ of L-^{14}C-leucine without FAMT] – 1) (25).

Efflux Measurements

Efflux measurements were performed as described previously (24). The cells were preloaded with 1 μM L-^{14}C-leucine (12.6 MBq/mmol) in Na$^+$-free HBSS for 10 min. The cells were then washed, and the efflux was initiated by incubating the cells for 1 min in Na$^+$-free HBSS medium with or without 40 μM nonradiolabeled test compounds, unless otherwise indicated. After incubation, the medium was collected. The radioactivity in the medium and the remaining radioactivity in cells were counted.

The kinetic parameters of FAMT-induced L-^{14}C-leucine efflux were determined on L-^{14}C-leucine efflux induced by extracellularly applied FAMT at concentrations of 1, 3, 10, 30, 50, 100, 300, and 1,000 μM for 1 min (24). To obtain FAMT-induced L-^{14}C-leucine efflux, the values for L-^{14}C-leucine efflux in the presence of extracellular FAMT were subtracted from those in the absence

of FAMT and expressed as the percentage of total radioactivity. The FAMT-induced L-^{14}C-leucine efflux was plotted against FAMT concentration and fitted to a Michaelis–Menten curve. K$_m$ and V$_{max}$ were determined using an Eadie–Hofstee plot.

Western Blot Analysis

The human cell lines were cultured for 2 d. The cells were lysed in buffer containing 50 mM Tris-Cl (pH 7.4), 120 mM NaCl, 20 mM NaF, 1 mM ethylenediaminetetraacetic acid, 6 mM ethylene glycol tetraacetic acid, 20 mM β-glycerophosphate, 1 mM dithiothreitol, 0.5 mM phenylmethanesulfonyl fluoride, 1 mM Na$_3$VO$_4$, 1% NP-40, and ethylenediaminetetraacetic acid–free protease inhibitor cocktail (Roche Diagnostics GmbH). The Western blot was conducted as described previously (22). Antihuman LAT1 polyclonal antibody (Trans Genic Inc.) and antihuman β-actin monoclonal antibody (Sigma Aldrich) were used at 1:10,000 dilution.

Statistical Analysis

All experiments were performed in 6–8 replications. The data are expressed as mean ± SEM. Statistical differences were determined using the unpaired Student t test. Differences were considered significant at a P value of less than 0.05.
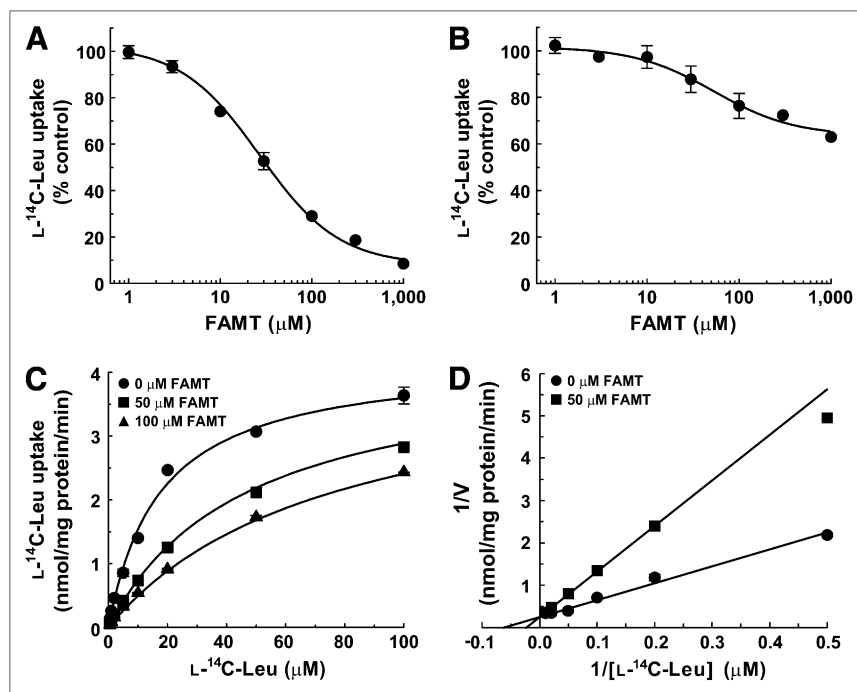
RESULTS

Inhibition of L-^{14}C-Leucine Uptake by FAMT in S2-LAT1 and S2-LAT2 Cells

The S2-LAT1 and S2-LAT2 cells were used to study the interaction of FAMT with human LAT1 and LAT2, respectively. The inhibition experiments were first performed to examine whether FAMT interacts with LAT1 and LAT2. FAMT prominently inhibited L-leucine uptake mediated by LAT1 but not by LAT2. As shown in Figure 2A, FAMT inhibited the uptake of L-^{14}C-leucine in a concentration-dependent manner with the IC$_{50}$ of 26.9 ± 1.1 μM in S2-LAT1 cells. In S2-LAT2 cells, in contrast, FAMT showed less inhibitory effect on the uptake of L-^{14}C-leucine (Fig. 2B). At 1,000 μM, FAMT inhibited L-^{14}C-leucine uptake by 37% in S2-LAT2 cells.

To determine whether the inhibition of LAT1 by FAMT is competitive, the effect of FAMT on the K$_m$ and V$_{max}$ of LAT1-mediated L-leucine uptake was examined. The uptake of L-^{14}C-leucine was measured at varied concentrations (1–100 μM) in the presence or absence of FAMT. As shown in Figure 2C, L-^{14}C-leucine uptake in the presence of 50 and 100 μM FAMT fitted to a Michaelis–Menten curve, with a K$_m$ and V$_{max}$ of 45.6 ± 1.6 μM and 4.1 ± 0.1 nmol/mg of protein/min, respectively, for 50 μM FAMT and 72.4 ± 6.7 μM and 4.4 ± 0.2 nmol/mg of protein/min, respectively, for 100 μM FAMT. K$_m$ and V$_{max}$ in the absence of FAMT were 15.5 ± 1.8 μM and 3.9 ± 0.2 nmol/mg of protein/min, respectively. These findings indicate that K$_m$ is increased by FAMT, with V$_{max}$ remaining unchanged. Double reciprocal plots confirmed that FAMT (50 μM) altered K$_m$ without changing V$_{max}$ (Fig. 2D), consistent with the competitive inhibition. K$_i$ value was calculated to be 29.5 ± 3.6 μM. Inhibition kinetics were not obtained for LAT2 because of the low level of inhibition.

FIGURE 2. Inhibitory effects of FAMT on L-^{14}C-leucine uptake in S2-LAT1 and S2-LAT2 cells. (A and B) Concentration-dependent inhibition of L-^{14}C-leucine uptake by FAMT in S2-LAT1 cells (A) and S2-LAT2 cells (B). Uptake of 1 μM L-^{14}C-leucine was measured in presence of varied concentrations of FAMT. Uptake values were fitted to inhibition curves. IC$_{50}$ of FAMT on LAT1-mediated L-^{14}C-leucine uptake was 26.9 μM. (C and D) Kinetics of inhibition of LAT1-mediated L-^{14}C-leucine uptake by FAMT. Uptake of L-^{14}C-leucine (1–100 μM) was measured in absence or presence of FAMT, and plotted against L-^{14}C-leucine concentration to fit to Michaelis–Menten curves (C). Double reciprocal plot analysis was performed on inhibitory effect of 50 μM FAMT (D). Two lines fit to competitive inhibition with FAMT's K$_i$ value of 29.5 μM. Leu = leucine.

L-^{14}C-Leucine Efflux Induced by FAMT

FAMT's competitive inhibition of LAT1-mediated L-^{14}C-leucine transport suggests that FAMT binds to the substrate binding site of LAT1. To determine whether FAMT is transported as a substrate of LAT1 after binding to the substrate binding site or is just a nontransportable inhibitor, we took advantage of the exchanger property of LAT1 (16,24,25). L-^{14}C-leucine was preloaded to S2-LAT1 cells, and the efflux of preloaded L-^{14}C-leucine from the cells induced by extracellularly applied FAMT was measured to determine whether FAMT is transported by LAT1 as its substrate. As shown in Figure 3A, extracellularly applied FAMT induced L-^{14}C-leucine efflux from S2-LAT1 cells more significantly than that measured in the absence of extracellular FAMT. The level of efflux induced by FAMT was similar to that induced by L-tyrosine, a well-characterized substrate of LAT1, suggesting that FAMT is transported by LAT1 in a manner similar to L-tyrosine. In contrast, the efflux of preloaded L-^{14}C-leucine from S2-LAT2 cells induced by FAMT was much less than that induced by L-tyrosine, which is a well-known substrate of LAT2 (Fig. 3B) (16,26).

The kinetic property of LAT1-mediated FAMT transport was then examined by analyzing the dependence of the efflux of preloaded L-^{14}C-leucine on the concentration of extracellularly applied FAMT (1–1,000 μM). The result showed that FAMT induced the efflux of preloaded L-^{14}C-leucine in a concentration-dependent manner (Fig. 3C). The efflux values became saturated at a higher concentration (300–1,000 μM) and fitted to a Michaelis–Menten curve (Fig. 3C). K$_m$ was 27.5 ± 0.9 μM, and the maximum L-^{14}C-leucine efflux rate (V$_{max}$) induced by FAMT was 27.7% ± 0.4% radioactivity/min. Kinetic parameters

of FAMT-induced L-^{14}C-leucine efflux were not obtained for LAT2 because of the low level of efflux.

Comparison of FAMT with Structurally Related Compounds and Other Amino Acid Tracers

To reveal the effect of fluorine moiety position on the interaction with LAT1 and LAT2, the inhibitory effect and efflux induction were examined on 2-FAMT, which has a fluorine at the 2 position in the aromatic ring (Fig. 1). As shown in Figures 4A and 4B, 2-FAMT inhibited the uptake of L-^{14}C-leucine in a concentration-dependent manner with an IC$_{50}$ of 28.8 ± 1.2 μM in S2-LAT1 cells, whereas 2-FAMT showed less inhibitory effect in S2-LAT2 cells. At 1,000 μM, 2-FAMT inhibited L-^{14}C-leucine uptake by 42% in S2-LAT2 cells. In the efflux experiments using S2-LAT1 and S2-LAT2 cells preloaded with L-^{14}C-leucine, extracellularly applied 2-FAMT induced a substantial level of L-^{14}C-leucine efflux from S2-LAT1 cells, whereas less L-^{14}C-leucine efflux was induced by 2-FAMT in S2-LAT2 cells (Figs. 4C and 4D).

Tyrosine-related compounds structurally related to FAMT and L-methionine were compared with FAMT in terms of the interaction with LAT1 and LAT2. As shown in Figure 5, 200 μM L-tyrosine, 3FT, 2FT, FET, and L-methionine strongly inhibited the uptake of L-^{14}C-leucine in both S2-LAT1 and S2-LAT2 cells in a similar manner. In contrast, FAMT, 2-FAMT, IMT, and AMT showed a strong inhibitory effect on LAT1 but less effect on LAT2.

In the efflux experiments, the transport of tyrosine-related compounds and L-methionine by LAT1 and LAT2 was compared with that of FAMT. As shown in Figure 6, L-tyrosine, FAMT, 2-FAMT, IMT, AMT, 3FT, 2FT, FET, and L-methionine induced efflux of preloaded L-^{14}C-leucine
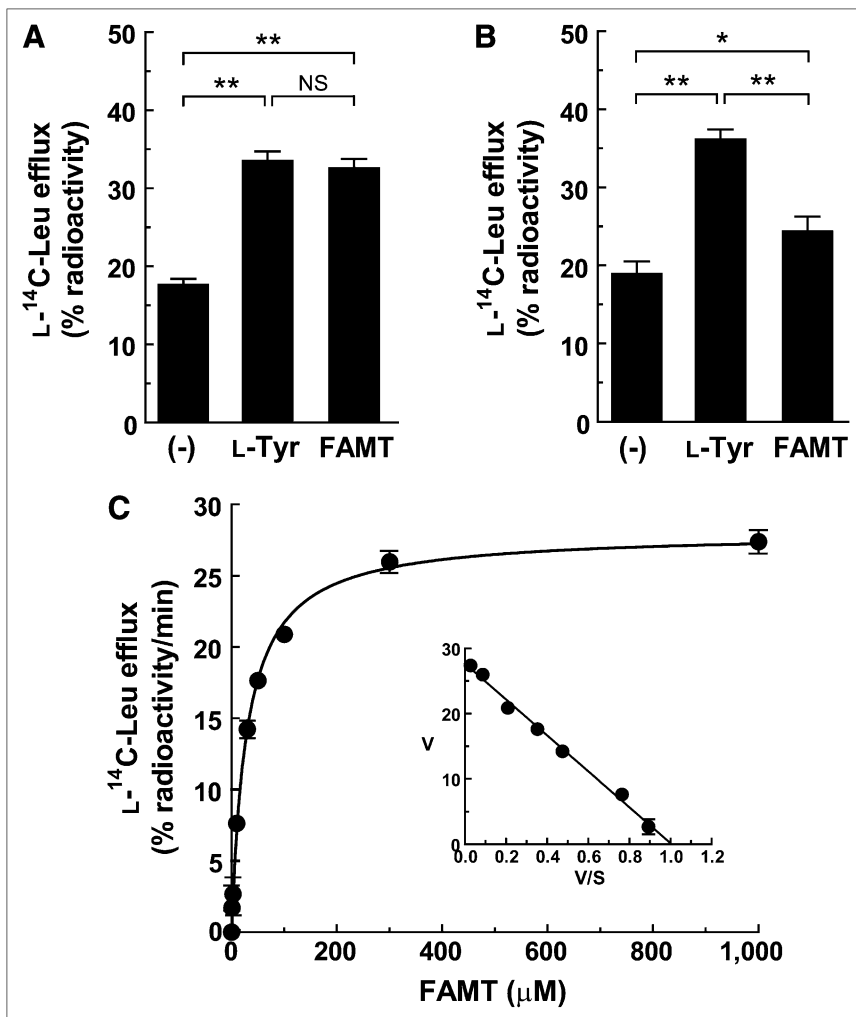
FIGURE 3. Efflux of L-^{14}C-leucine induced by FAMT in S2-LAT1 and S2-LAT2 cells. (A and B) Efflux of preloaded L-^{14}C-leucine from S2-LAT1 cells (A) and S2-LAT2 cells (B) in absence ((−)) or presence of 40 μM L-tyrosine and FAMT. (C) Concentration dependence of effect of FAMT on induction of L-^{14}C-leucine efflux from S2-LAT1 cells. Efflux of preloaded L-^{14}C-leucine from S2-LAT1 cells was measured for 1 min in presence of extracellularly applied FAMT. Radioactivity of L-^{14}C-leucine released from cells in presence of FAMT was subtracted from that in absence of FAMT ((−) in A). Efflux values were fit to Michaelis–Menten curve. Inset shows Eadie–Hofstee plot of L-^{14}C-leucine efflux, which was used to determine kinetic parameters. Apparent K_m of 27.5 μM and V_{max} of 27.7% radioactivity/min were obtained. *$P < 0.05$. **$P < 0.01$. Leu = leucine; NS = not significant.

through LAT1 at similar levels, whereas the efflux of L-^{14}C-leucine mediated by LAT2 was much less for FAMT, 2-FAMT, IMT, and AMT, compared with L-tyrosine, 3FT, 2FT, FET, and L-methionine.

Correlation of FAMT Transport and LAT1 Expression

To confirm the role of LAT1 in FAMT uptake, FAMT transport rate and LAT1 expression level were compared in human cell lines. The FAMT transport rate was measured as the rate of efflux of preloaded L-^{14}C-leucine induced by 40 μM FAMT, and LAT1 protein expression level was evaluated by Western blot. As shown in Figure 7, among human cell lines examined in this study, HEK 293 cells exhibited the lowest LAT1 expression level and the lowest FAMT transport rate. HeLa S3, HEp-2, and H520 cells showed a high level of LAT1 expression and a high FAMT transport rate. T24, MIA PaCa-2, and DLD-1 were in the medium range of LAT1 expression and FAMT transport.

DISCUSSION

In this study, using cell lines stably expressing human LAT1 (S2-LAT1 cells) or human LAT2 (S2-LAT2 cells),

we investigated the mechanism of FAMT accumulation. FAMT prominently inhibited LAT1-mediated L-^{14}C-leucine uptake in a competitive manner (Fig. 2) and stimulated the LAT1-mediated efflux of preloaded L-^{14}C-leucine (Figs. 3A and 3C), indicating that FAMT binds to the substrate-binding site of LAT1 and is transported by LAT1 as its substrate. The affinity of FAMT evaluated on the basis of K_i for inhibiting L-^{14}C-leucine uptake and K_m for inducing L-^{14}C-leucine efflux is similar to that of known LAT1 substrates such as L-tyrosine, L-leucine, and L-methionine (12,25), suggesting that FAMT is transported by LAT1 as efficiently as endogenous substrates. In contrast, FAMT weakly inhibited LAT2-mediated L-^{14}C-leucine uptake (Fig. 2B) and only slightly induced LAT2-mediated L-^{14}C-leucine efflux (Fig. 3B), indicating that FAMT is hardly transported by LAT2. Therefore, FAMT is able to discriminate 2 closely related system L transporters, LAT1 and LAT2, and is selectively transported by LAT1.

FAMT is an L-tyrosine derivative modified by adding a methyl group at the α-carbon and a fluorine moiety at the 3 position of the aromatic ring (Fig. 1) (6). Although L-tyrosine is recognized by both LAT1 and LAT2 as a substrate, FAMT is
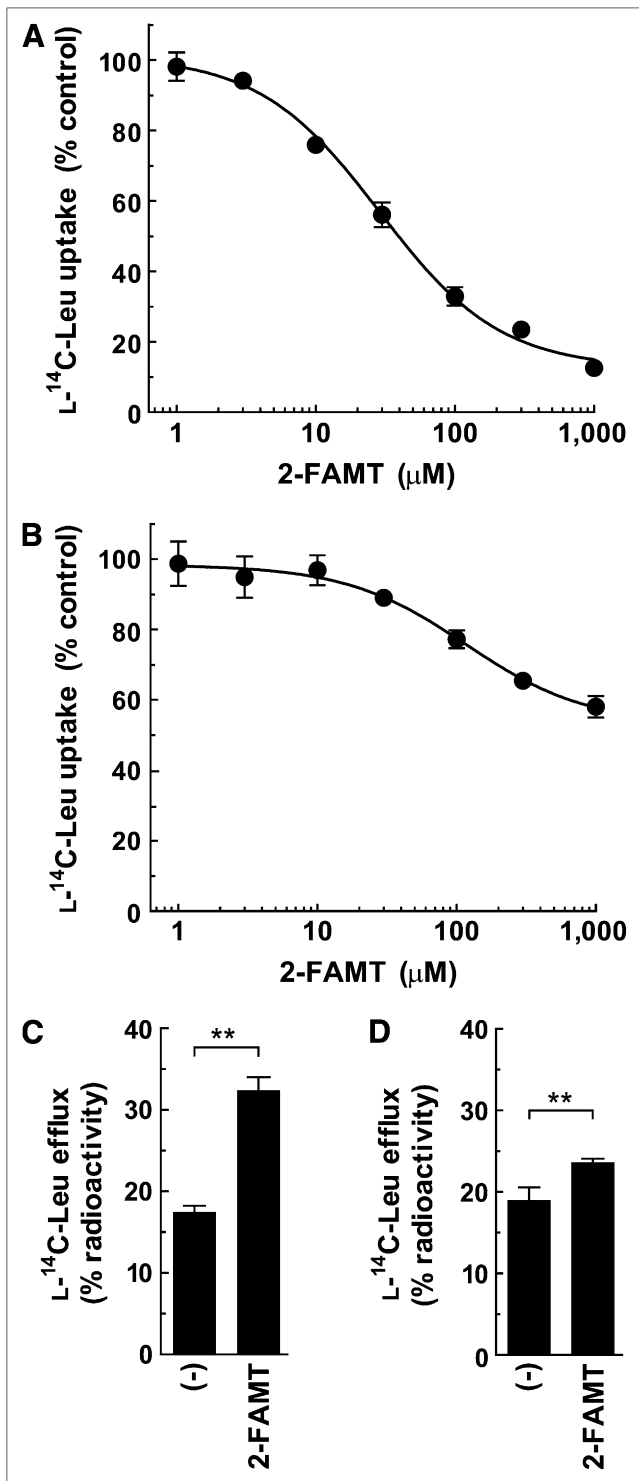
FIGURE 5. Inhibitory effects of tyrosine-related compounds and L-^{14}C-methionine on L-^{14}C-leucine uptake in S2-LAT1 and S2-LAT2 cells. Uptake of 1 μM L-^{14}C-leucine was measured for 1 min in absence ((−)) or presence of 200 μM tyrosine-related compounds and L-methionine in S2-LAT1 and S2-LAT2 cells. Uptake values were expressed as percentage of control L-^{14}C-leucine uptake measured in absence of inhibitors. Leu = leucine.

selective to LAT1 (Figs. 2 and 3). 2-FAMT, which has a fluorine at the 2 position, showed properties similar to FAMT in the effect on LAT1 and LAT2 in terms of inhibition of L-^{14}C-leucine uptake and induction of L-^{14}C-leucine efflux (Fig. 4). 3FT and 2FT that had a fluorine moiety but lacked an α-methyl group (Fig. 1) were transported by both LAT1 and LAT2 in a manner similar to L-tyrosine (Figs. 5 and 6). AMT lacking a fluorine was still LAT1-selective (Figs. 5 and 6). Thus, the presence of a fluorine moiety and its position in the aromatic ring do not affect the interaction with LAT1 and LAT2. In contrast, the presence of the α-methyl group is critical for LAT1 selectivity. IMT and AMT, as well as FAMT and 2-FAMT—which have an α-methyl group (Fig. 1)—were well

FIGURE 6. Efflux of L-^{14}C-leucine induced by tyrosine-related compounds and L-methionine in S2 LAT1 and S2-LAT2 cells. Efflux of preloaded L-^{14}C-leucine from S2-LAT1 and S2-LAT2 cells was measured for 1 min in absence or presence of extracellularly applied indicated compounds (40 μM). Radioactivity released from cells in presence of test compounds was subtracted from radioactivity in their absence. Leu = leucine.

FIGURE 4. Interaction of 2-FAMT with LAT1 and LAT2. (A and B) Concentration-dependent inhibition of L-^{14}C-leucine uptake by 2-FAMT in S2-LAT1 cells (A) and S2-LAT2 cells (B). Uptake of 1 μM L-^{14}C-leucine was measured in presence of varied concentrations of 2-FAMT. Uptake values were fitted by nonlinear regression to inhibition curve. IC$_{50}$ of 2-FAMT on LAT1-mediated L-^{14}C-leucine uptake was 28.8 μM. (C and D) Efflux of preloaded L-^{14}C-leucine from S2-LAT1 cells (C) and S2-LAT2 cells (D) in absence ((−)) or presence of 40 μM 2-FAMT. **$P < 0.01$. Leu = leucine.
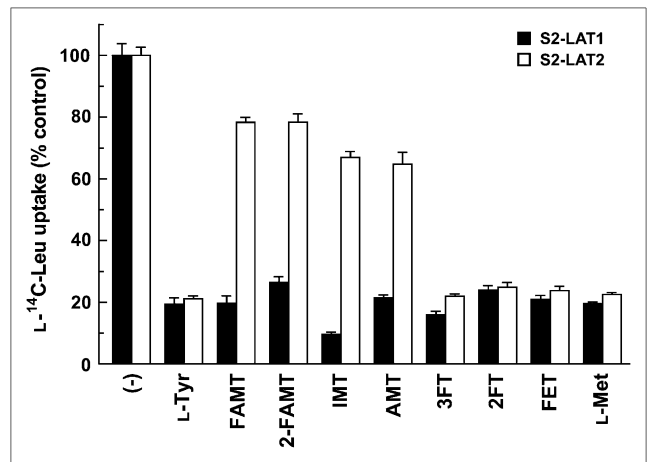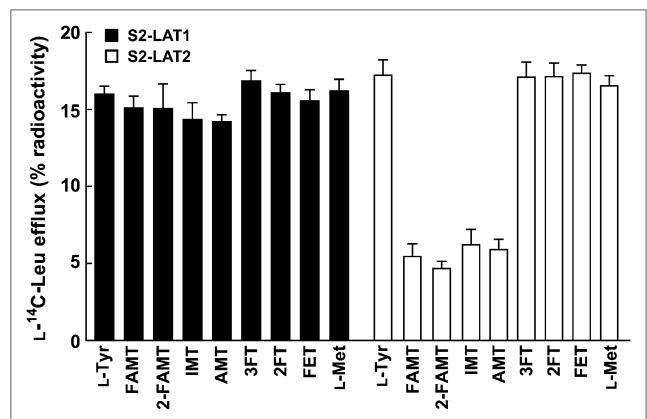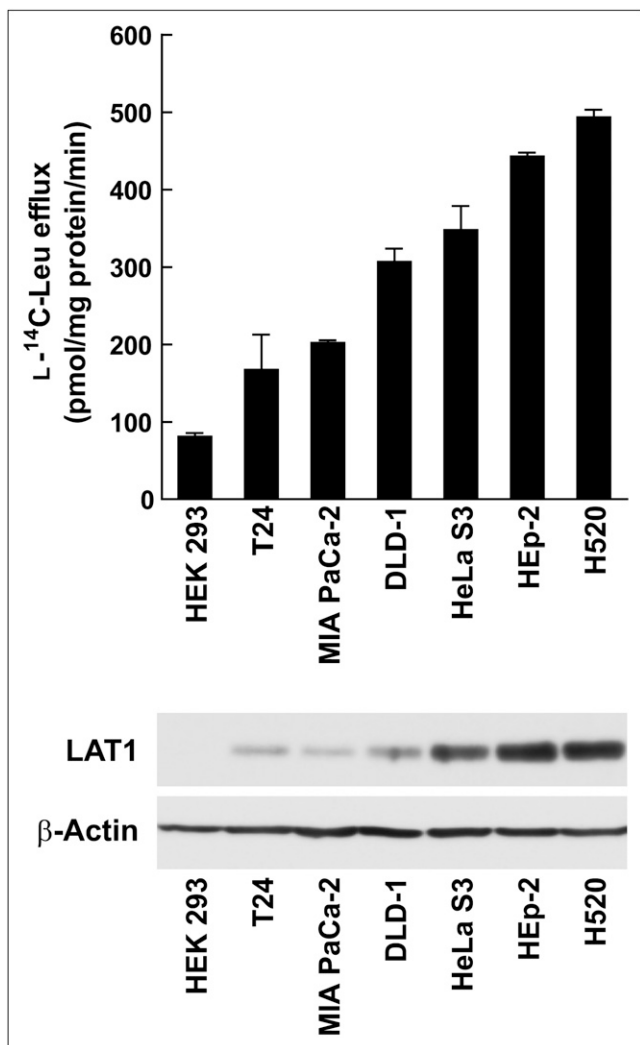
FIGURE 7. Comparison of FAMT transport rate and LAT1 expression level in human cell lines. FAMT transport rate (top) and LAT1 expression level (bottom) were determined in human cell lines HEK 293, T24, MIA PaCa-2, DLD-1, HeLa S3, HEp-2, and H520. FAMT transport rate was evaluated by measuring efflux of preloaded L-^{14}C-leucine (1 min) induced by 40 μM FAMT. Radioactivity of L-^{14}C-leucine released from cells in presence of FAMT was subtracted from radioactivity in absence of FAMT. Western blot analysis of LAT1 and β-actin were conducted on total cell lysate of indicated human cell lines. Leu = leucine.

transported by LAT1, whereas they interacted less with LAT2 (Figs. 5 and 6). Therefore, the α-methyl group but not fluorine is the key moiety for FAMT to be LAT1-selective. Consistent with this, we previously showed that α-methyl phenylalanine and α-methyl 3,4-dihydroxyphenylalanine and AMT inhibited L-^{14}C-leucine uptake mediated by LAT1, but they had less of an effect on LAT2 (22,24,25). Moreover, in the amphibian oocyte expression system, we observed that L-3-^{125}I-α-methyl tyrosine (^{125}I-IMT) is transported by LAT1 but not by LAT2 (27).

Besides LAT1 and LAT2, 2 additional system L transporters, LAT3 and LAT4, were identified in the transporter family distinct from that of LAT1 and LAT2 (14,15). There are some reports indicating that LAT3 and LAT4 are not only expressed in normal tissues but also upregulated in some cancers (14,28). LAT3 and LAT4 mainly transport L-phenylalanine, L-methionine, and branched chain amino acids, whereas they interact less with L-tyrosine. It was also shown that AMT does not inhibit LAT4-mediated transport (15). We furthermore confirmed that AMT does not inhibit LAT3-mediated L-leucine transport using a *Xenopus* oocyte expression system (data not shown). The fact that L-tyrosine and AMT interact less with LAT3 and LAT4 suggests that FAMT would not be a substrate of LAT3 and LAT4. Thus, FAMT is specific to LAT1 among system L transporters.

Other candidate transporters that might interact with aromatic amino acid PET tracers are system T, B^0, and $B^{0,+}$ (Table 1). We showed, in a previous study, that system T transporter TAT1 does not transport α-methyl amino acids (29), suggesting that FAMT is not transported by system T because of its α-methyl moiety. System B^0 and $B^{0,+}$ transporters were previously suggested to somewhat transport a SPECT tracer, L-3-^{123}I-α-methyl tyrosine (^{123}I-IMT) (30,31). System B^0, a Na^+-dependent broad-scope neutral amino acid transporter, is present on the apical membrane of renal proximal tubules and small intestine and responsible for the absorption of neutral amino acids from the lumen (26). Thus, system B^0 was proposed to contribute to the renal accumulation of ^{123}I-IMT and ^{125}I-IMT (31). Although direct interaction of FAMT and IMT with system B^0 transporters was not examined, it is possible that the accumulation of ^{18}F-FAMT in kidney in PET is also due to the reabsorption of ^{18}F-FAMT from tubular lumen to tubular epithelial cells via system B^0 transporters. System $B^{0,+}$ transporter $ATB^{0,+}$, which mediates Na^+-dependent broad-scope transport of neutral and basic amino acids, was reported to be expressed mainly in the lung, trachea, and salivary gland and at a lower level in the mammary gland, stomach, and pituitary gland in humans (32). However, the significance of system $B^{0,+}$ in ^{123}I-IMT SPECT is not considered to be high because of the low background accumulation of ^{123}I-IMT in tissues expressing $ATB^{0,+}$ and because of the low contribution of system $B^{0,+}$ to total ^{123}I-IMT uptake in tumor cells. $B^{0,+}$-mediated uptake accounts for approximately 15% of total ^{123}I-IMT uptake in glioma cells, whereas approximately 70% of the uptake is due to system L (30). Similar to ^{123}I-IMT SPECT, the contribution of system $B^{0,+}$ to ^{18}F-FAMT PET would not be high, considering the low accumulation of ^{18}F-FAMT in tissues expressing systems $B^{0,+}$ (8). It was previously reported that the uptake of 3-*O*-methyl-6-^{18}F-fluoro-L-dopa was not correlated with LAT1 messenger RNA level (28). In the present study, we compared FAMT transport rate with LAT1 protein level, which reflects more directly transport functions, and we obtained a good correlation between them (Fig. 7). This observation at least supports the importance of LAT1 for the cellular uptake of FAMT, although the idea that FAMT is specific to LAT1 among transporters of plasma membrane needs to be confirmed experimentally.

Among amino acid analogs used for PET tracers tested in this study, only FAMT prefers LAT1 to LAT2. L-methionine,

TABLE 1
Amino Acid Transporters for Uptake of Amino Acid PET/SPECT Tracers

PET/SPECT tracer	Amino acid transport system	Transporter	Reference
FAMT	L	LAT1	This study
IMT	L	LAT1	(27), this study
	B⁰		(31)
	B⁰,⁺		(30)
L-Tyr	L	LAT1, LAT2	(12,13), this study
	T	TAT1	(29)
	B⁰	B⁰AT1	(26)
	B⁰,⁺	ATB⁰,⁺	(26)
2FT	L	LAT1, LAT2	(33), this study
	B⁰		(38)
	B⁰,⁺		(38)
FET	L	LAT1, LAT2	(38), this study
	B⁰		(38)
	B⁰,⁺		(38)
L-Met	L	LAT1, LAT2, LAT3, LAT4	(12–15), this study
	A	SNAT1, SNAT2, SNAT4	(26)
	ASC	ASCT2	(26)
	y⁺L	y⁺LAT1, y⁺LAT2	(26)
	b⁰,⁺	b⁰,⁺AT	(26)
	B⁰	B⁰AT1, B⁰AT2	(26)
	B⁰,⁺	ATB⁰,⁺	(26)

ATB$^{0,+}$ = amino acid transporter B$^{0,+}$; SNAT = sodium-coupled neutral amino acid transporter.

L-tyrosine, FET, 3FT, and 2FT are all transported by both LAT1 and LAT2 (Figs. 5 and 6) (33). The uptake of ^{11}C-MET is recognized in the pancreas, liver, and inflammatory lesions (4,34,35). Relatively strong signals of ^{11}C-MET in these tissues may be due to protein incorporation, because pancreatic accumulation is also found for ^{11}C-tyrosine and ^{18}F-2FT, which are incorporated into proteins (35–37). Another possible explanation for the uptake of ^{11}C-MET in nontumor tissues and inflammatory lesions is the multiple transport systems involved in L-methionine transport. L-methionine is a substrate of systems L, A, ASC, y$^+$L, b$^{0,+}$, B^0, and B$^{0,+}$ (Table 1) (16,26,38). ^{18}F-FET and ^{18}F-FAMT show lower physiologic backgrounds and accumulate more selectively to malignant tumors, probably because aromatic amino acids are transported by more limited transport systems than L-methionine. ^{18}F-FET, however, accumulates in reactive astrocytes around brain abscesses and shows physiologic background uptake in skeletal muscle (5,35,39). Some investigators have proposed that ^{18}F-FET is taken up by skeletal muscle via LAT2 expressed in the muscle (5,40). Consistent with this proposal, ^{18}F-FAMT and ^{123}I-IMT, both specific to LAT1 and not transported by LAT2, do not accumulate in skeletal muscle in PET and SPECT, respectively (8,40).

CONCLUSION

In this study, by means of an in vitro transport assay using established mammalian cell lines stably expressing human LAT1 and human LAT2, we have shown that FAMT is a high-affinity substrate of LAT1. Distinct from the other amino acid PET tracers, FAMT is selective to LAT1 and interacts less with LAT2 because of its α-methyl moiety. This property of FAMT contributes to highly tumor-specific accumulation of ^{18}F-FAMT in PET.

DISCLOSURE STATEMENT

ACKNOWLEDGMENTS

REFERENCES

1. Plathow C, Weber WA. Tumor cell metabolism imaging. *J Nucl Med*. 2008;49 (suppl 2):43S–63S.

2. Cook GJ, Maisey MN, Fogelman I. Normal variants, artefacts and interpretative pitfalls in PET imaging with 18-fluoro-2-deoxyglucose and carbon-11 methionine. *Eur J Nucl Med.* 1999;26:1363–1378.

3. Jager PL, Vaalburg W, Pruim J, de Vries EG, Langen KJ, Piers DA. Radiolabeled amino acids: basic aspects and clinical applications in oncology. *J Nucl Med.* 2001;42:432–445.

4. Deloar HM, Fujiwara T, Nakamura T, et al. Estimation of internal absorbed dose of L-[methyl-11C]methionine using whole-body positron emission tomography. *Eur J Nucl Med.* 1998;25:629–633.

5. Pauleit D, Floeth F, Herzog H, et al. Whole-body distribution and dosimetry of O-(2-18F-fluoroethyl)-L-tyrosine. *Eur J Nucl Med Mol Imaging.* 2003;30:519–524.

6. Tomiyoshi K, Amed K, Muhammad S, et al. Synthesis of isomers of 18F-labelled amino acid radiopharmaceutical: position 2- and 3-L-18F-α-methyltyrosine using a separation and purification system. *Nucl Med Commun.* 1997;18:169–175.

7. Inoue T, Shibasaki T, Oriuchi N, et al. 18F-α-methyl tyrosine PET studies in patients with brain tumors. *J Nucl Med.* 1999;40:399–405.

8. Inoue T, Koyama K, Oriuchi N, et al. Detection of malignant tumors: wholebody PET with fluorine 18 α-methyl tyrosine versus FDG–preliminary study. *Radiology.* 2001;220:54–62.

9. Kaira K, Oriuchi N, Otani Y, et al. Fluorine-18-α-methyltyrosine positron emission tomography for diagnosis and staging of lung cancer: a clinicopathologic study. *Clin Cancer Res.* 2007;13:6369–6378.

10. Kaira K, Oriuchi N, Shimizu K, et al. 18F-FMT uptake seen within primary cancer on PET helps predict outcome of non-small cell lung cancer. *J Nucl Med.* 2009;50:1770–1776.

11. Kaira K, Oriuchi N, Shimizu K, et al. Evaluation of thoracic tumors with 18F-FMT and 18F-FDG PET-CT: a clinicopathological study. *Int J Cancer.* 2009; 124:1152–1160.

12. Kanai Y, Segawa H, Miyamoto K, Uchino H, Takeda E, Endou H. Expression cloning and characterization of a transporter for large neutral amino acids activated by the heavy chain of 4F2 antigen (CD98). *J Biol Chem.* 1998;273:23629–23632.

13. Segawa H, Fukasawa Y, Miyamoto K, Takeda E, Endou H, Kanai Y. Identification and functional characterization of a Na+-independent neutral amino acid transporter with broad substrate selectivity. *J Biol Chem.* 1999;274:19745–19751.

14. Babu E, Kanai Y, Chairoungdua A, et al. Identification of a novel system L amino acid transporter structurally distinct from heterodimeric amino acid transporters. *J Biol Chem.* 2003;278:43838–43845.

15. Bodoy S, Martin L, Zorzano A, Palacin M, Estevez R, Bertran J. Identification of LAT4, a novel amino acid transporter with system L activity. *J Biol Chem.* 2005;280: 12002–12011.

16. Kanai Y, Endou H. Heterodimeric amino acid transporters: molecular biology and pathological and pharmacological relevance. *Curr Drug Metab.* 2001;2:339–354.

17. Fuchs BC, Bode BP. Amino acid transporters ASCT2 and LAT1 in cancer: partners in crime? *Semin Cancer Biol.* 2005;15:254–266.

18. Nawashiro H, Otani N, Shinomiya N, et al. L-type amino acid transporter 1 as a potential molecular target in human astrocytic tumors. *Int J Cancer.* 2006;119: 484–492.

19. Kaira K, Oriuchi N, Imai H, et al. Prognostic significance of L-type amino acid transporter 1 expression in resectable stage I-III nonsmall cell lung cancer. *Br J Cancer.* 2008;98:742–748.

20. Kaira K, Oriuchi N, Imai H, et al. Prognostic significance of L-type amino acid transporter 1 (LAT1) and 4F2 heavy chain (CD98) expression in stage I pulmonary adenocarcinoma. *Lung Cancer.* 2009;66:120–126.

21. Ooi T, Takeuchi M, Kameda M, Maruoka K. Practical catalytic enantioselective synthesis of α,α-dialkyl−α−amino acids by chiral phase-transfer catalysis. *J Am Chem Soc.* 2000;122:5228–5229.

22. Morimoto E, Kanai Y, Kim DK, et al. Establishment and characterization of mammalian cell lines stably expressing human L-type amino acid transporters. *J Pharmacol Sci.* 2008;108:505–516.

23. Oda K, Hosoda N, Endo H, et al. L-type amino acid transporter 1 inhibitors inhibit tumor cell growth. *Cancer Sci.* 2010;101:173–179.

24. Kim DK, Kanai Y, Choi HW, et al. Characterization of the system L amino acid transporter in T24 human bladder carcinoma cells. *Biochim Biophys Acta.* 2002;1565:112–121.

25. Uchino H, Kanai Y, Kim DK, et al. Transport of amino acid-related compounds mediated by L-type amino acid transporter 1 (LAT1): insights into the mechanisms of substrate recognition. *Mol Pharmacol.* 2002;61:729–737.

26. Bröer S. Amino acid transport across mammalian intestinal and renal epithelia. *Physiol Rev.* 2008;88:249–286.

27. Shikano N, Kanai Y, Kawai K, et al. Isoform selectivity of 3-125I-iodo-α-methyl-L-tyrosine membrane transport in human L-type amino acid transporters. *J Nucl Med.* 2003;44:244–246.

28. Haase C, Bergmann R, Fuechtner F, Hoepping A, Pietzsch J. L-type amino acid transporters LAT1 and LAT4 in cancer: Uptake of 3-O-methyl-6-18F-fluoro-L-dopa in human adenocarcinoma and squamous cell carcinoma in vitro and in vivo. *J Nucl Med.* 2007;48:2063–2071.

29. Kim DK, Kanai Y, Chairoungdua A, Matsuo H, Cha SH, Endou H. Expression cloning of a Na+-independent aromatic amino acid transporter with structural similarity to H+/monocarboxylate transporters. *J Biol Chem.* 2001;276:17221–17228.

30. Riemann B, Kopka K, Stogbauer F, et al. Kinetic parameters of 3-[123I]iodo-L-α-methyl tyrosine ([123I]IMT) transport in human GOS3 glioma cells. *Nucl Med Biol.* 2001;28:293–297.

31. Shikano N, Kawai K, Nakajima S, et al. Renal accumulation and excretion of radioiodinated 3-iodo-α-methyl-L-tyrosine. *Ann Nucl Med.* 2004;18:263–270.

32. Sloan JL, Mager S. Cloning and functional expression of a human Na+ and Cl-dependent neutral and cationic amino acid transporter B0,+. *J Biol Chem.* 1999;274:23740–23745.

33. Lahoutte T, Caveliers V, Camargo SM, et al. SPECT and PET amino acid tracer influx via system L (h4F2hc-hLAT1) and its transstimulation. *J Nucl Med.* 2004;45:1591–1596.

34. Rau FC, Weber WA, Wester HJ, et al. O-(2-[18F]fluoroethyl)-L-tyrosine (FET): a tracer for differentiation of tumour from inflammation in murine lymph nodes. *Eur J Nucl Med Mol Imaging.* 2002;29:1039–1046.

35. Salber D, Stoffels G, Pauleit D, et al. Differential uptake of O-(2-18F-fluoroethyl)-L-tyrosine, L-3H-methionine, and 3H-deoxyglucose in brain abscesses. *J Nucl Med.* 2007;48:2056–2062.

36. Ishiwata K, Kubota K, Murakami M, et al. Re-evaluation of amino acid PET studies: can the protein synthesis rates in brain and tumor tissues be measured in vivo? *J Nucl Med.* 1993;34:1936–1943.

37. Ishiwata K, Enomoto K, Sasaki T, et al. A feasibility study on L-[1-carbon-11] tyrosine and L-[methyl-carbon-11]methionine to assess liver protein synthesis by PET. *J Nucl Med.* 1996;37:279–285.

38. Langen KJ, Jarosch M, Muhlensiepen H, et al. Comparison of fluorotyrosines and methionine uptake in F98 rat gliomas. *Nucl Med Biol.* 2003;30:501–508.

39. Stöber B, Tanase U, Herz M, Seidl C, Schwaiger M, Senekowitsch-Schmidtke R. Differentiation of tumour and inflammation: characterisation of [methyl-3H] methionine (MET) and O-(2-[18F]fluoroethyl)-L-tyrosine (FET) uptake in human tumour and inflammatory cells. *Eur J Nucl Med Mol Imaging.* 2006;33: 932–939.

40. Pauleit D, Floeth F, Tellmann L, et al. Comparison of O-(2-18F-fluoroethyl)-L-tyrosine PET and 3-123I-iodo-α-methyl-L-tyrosine SPECT in brain tumors. *J Nucl Med.* 2004;45:374–381.